PB-215 855

COMPARISON OF KINETIC AND DIFFUSIONAL MODELS FOR SOLID-LIQUID REACTIONS

C. Y. Wen

West Virginia University
Morgantown, West Virginia

1967

DISTRIBUTED BY:

NTIS

National Technical Information Service
U. S. DEPARTMENT OF COMMERCE
5285 Port Royal Road, Springfield Va. 22151

WP00699

PB 215 855

COMPARISON OF KINETIC AND DIFFUSIONAL MODELS FOR SOLID-LIQUID REACTIONS

A Report to

Federal Water Pollution Control Administration
U.S. Department of the Interior

on

"Mass Transfer and Chemical Reaction in Water Pollution"

under

Grant No. WP 00699

Reproduced by
NATIONAL TECHNICAL
INFORMATION SERVICE
U S Department of Commerce
Springfield VA 22151

by

C. Y. Wen
West Virginia University
Morgantown, West Virginia
1967

I

COMPARISON OF KINETIC AND DIFFUSIONAL MODELS FOR SOLID-LIQUID REACTIONS

by

C. Y. Wen
West Virginia University

ABSTRACT

A comparison of the kinetic and diffusional models for solid-liquid reactions occuring in a spherical particle is presented. The similarities and differences of the unreacted-core shrinking model and the homogeneous model are examined in light of the rate-controlling factors. In view of the similarity of the two models, it is shown that erroneous conclusions in regard to the mechanism and the activation energies may be drawn from an analysis of the experimental data. A more versatile model is developed in order to augment the two models so that wider varieties of solid-liquid reaction systems may be treated. The concept of effectiveness factors in solid-liquid reactions is introduced and the influence of diffusion is ascertained. The present study presents a better phenomenological understanding of the mechanism of mass transfer and chemical reaction occuring in water pollution between liquid and solid.

COMPARISON OF KINETIC AND DIFFUSIONAL MODELS FOR SOLID-LIQUID REACTIONS

The mechanism by which components from a solid particle react and diffuse into liquid occuring in water pollution can be studied based on various phenomenological models. Many of these models are developed in the chemical and metallurgical fields associated with solid-fluid reaction systems. In a great majority of instances, the analysis of these solid-liquid reactions have been based on the "unreacted-core shrinking model" as shown by Yagi and Kunii (2). This model is acceptable because the porosity of the unreacted solid is usually very small meaning the solid is practically impervious to the liquid reactarts, and the reaction will occur at the surface of the solid or at the interface between the unreacted solid and the porous product layer. This model is also applicable when the chemical reaction rate is very rapid and the diffusion is sufficiently slow. The zone of reaction in such a case will be narrowly confined to the interface between the unreacted solid and the product. On the other hand, solid-liquid reactions in water pollution may also involve cases in which the solid contains enough voidage so that the liquid reactant can diffuse freely into the interior of the solid. Under such circumstances, the "unreacted-core shrinking model" is no longer applicable. In such cases, the reactions between liquid and solid may be viewed as occuring homogeneously throughout the solid to produce a gradual variation in solid reactant concentration in all parts of the particle. Therefore, another model, which we shall call the "homogeneous model", is needed for the analysis of porous solid-liquid reactions. Here, the

solid may be considered as an ensemble of small lumps of reactant distributed uniformly throughout the solid phase. The effective diffusivities of liquid components through the solid are considered large and are invarient during the reaction. Reactions occuring in ion-exchange resins for example can also be treated based on the "homogeneous" model.

Because of the mathematical difficulty, the homogeneous model has not been applied to solid-liquid reactions except for some special cases. Ausman and Watson (1) using a pseudo-steady state approximation for gas concentration distribution and a first order reaction with respect to the gaseous reactant, obtained a general solution for a solid-gas reaction in a spherical particle based on the homogeneous model. However, the results of their analysis have not been utilized by other investigators because the treatment involves a graphical solution of one of the differential equations. In actuality, however, solid-liquid reactions cannot be completely described either by the unreacted-core shrinking model or by the homogeneous model. The majority of cases belonging to this class of solid-liquid reactions are probably an intermediate of these two models. It seems therefore worthwhile to examine and to clarify the relation of these models and to provide a possibility of developing a more versatile model applicable under a wide variety of conditions occuring in water pollution.

In the following discussion, we shall present a general model for solid-liquid reactions and show that the unreacted-core shrinking

model and the homogeneous model are the special cases of the general model. In this connection, an analytical solution for the general model will be obtained and a comparison and an examination of the various models will be presented. In addition, the concept of the effectiveness factors developed in catalytic reactions will be extended to solid-liquid reactions based on these models. The effects of the diffusion into the solid and across the liquid film around the particle on these effectiveness factors will be shown.

A GENERAL MODEL FOR SOLID-LIQUID REACTIONS

Let us consider a class of solid-liquid reactions represented by

$$aA(l) + S(s) \rightarrow \text{products}.$$

A material balance for liquid reactant A and solid reactant S can be written as

$$\varepsilon \frac{\partial C_A}{\partial t} = \nabla (D_{eA} \nabla C_A) - r_A \tag{1}$$

$$\frac{\partial C_S}{\partial t} = - r_S \tag{2}$$

where r_A and r_S are stoichiometrically related by $r_A = a r_S$, and are the rates of reaction for liquid component A and for solid reactant, S, respectively. The boundary conditions are

$$\left.\begin{aligned} D_{eA} \nabla C_A &= k_{mA} (C_{Ao} - C_A) && \text{at the solid surface} \\ \nabla C_A &= 0 && \text{at the center} \end{aligned}\right\} \tag{3}$$

$$C_S = C_{So} \qquad \text{at } t = 0$$

D_{eA} is the effective diffusivity of component A through the solid, C_A and C_{Ao} are the concentrations of A in the solid and in the bulk liquid phase, respectively. k_{mA} is the mass transfer coefficient of component A from the bulk of the liquid phase to the solid surface across the liquid film, C_S is the solid reactant concentration at time t, and C_{So} is the initial solid reactant concentration. A solution of the above equations for a spherical particle is given below under the following assumptions.

(1) Pseudo steady-state approximation for A is valid, or $\epsilon \frac{\partial C_A}{\partial t} = 0$. The pseudo steady state approximation has been shown to be valid for most solid-liquid reactions when concentration of A is small.

(2) The rate of reaction is independent of the solid reactant concentration but is first order with respect to the reactant, A. Thus, $r_A = ak_v C_{So}(C_A - C_A^*)$ where C_A^* is the equilibrium concentration of A, a is the number of moles of A that will react with one mole of solid S, and k_v is the volumetric reaction rate constant.

Since the reaction is faster near the surface than in the interior of the particle, after a certain time the solid reactant near the surface will be completely exhausted forming an inert product layer (ash layer) as illustrated in Fig. 1. We shall designate the period of reaction prior to the formation of the ash layer as the First Stage, and the period following the ash layer formation as the Second Stage. For convenience, we shall use C'_A and D'_{eA} to denote the concentration and the effective diffusivity, respectively, of A in the solid during the first stage of the reaction and in the reaction zone during the second stage of the reaction. We shall use C_A and D_{eA} to denote the concentration and the effective diffusivity of A in the product ash layer during the second stage of reaction. We shall assume that D'_{eA} and D_{eA} are constant throughout the reaction.

(a) The First Stage Reaction

A schematic diagram of the reacting particle during the first stage is shown in Fig. 2. The material balance and the boundary conditions given in Equations (1), (2), and (3) now become

$$0 = D'_{eA}\left(\frac{d^2C'_A}{dr^2} + \frac{2}{r}\frac{dC'_A}{dr}\right) - ak_vC_{So}\,(C'_A - C^*_A) \tag{5}$$

$$\frac{\partial C_S}{\partial t} = -k_vC_{So}\,(C'_A - C^*_A) \tag{6}$$

$$\left.\begin{aligned} D'_{eA}\frac{dC'_A}{dr} &= k_{mA}\,(C_{Ao} - C'_A) \qquad \text{at } r = R \\ \frac{dC'_A}{dr} &= 0 \qquad\qquad\qquad\quad \text{at } r = 0 \end{aligned}\right\} \tag{7}$$

The concentration profile of A in the particle can be obtained as

$$\frac{C'_A - C^*_A}{C_{Ao} - C^*_A} = \frac{1}{\theta_{vc}}\,\frac{\sinh(\phi'_v\xi)}{\xi\sinh\phi'_v} \tag{8}$$

where $\xi = \dfrac{r}{R}$, $\phi'_v = R\sqrt{\dfrac{ak_vC_{So}}{D'_{eA}}}$,

$$\theta_{vc} = 1 + \frac{1}{N'_{Sh}}\,(\phi'_v\coth\phi'_v - 1), \text{ and } N'_{Sh} = \frac{k_{mA}R}{D'_{eA}}$$

In Fig. 3, the effect of the variation of ϕ'_v on the concentration profile of reactant A is shown for $N'_{Sh} = \infty$. For ϕ'_v larger than 50, the rate of chemical reaction becomes much faster than the diffusion through the solid, and consequently, the reaction takes place before A can diffuse into the interior of the particle. The variation in the solid reactant concentration can be found from

$$C_S = C_{So} - \int_0^t k_vC_{So}(C'_A - C^*_A)\,dt, \text{ as}$$

$$\frac{C_S}{C_{So}} = 1 - \frac{\sinh(\phi'_v \xi)}{\xi \sinh \phi'_v} \frac{\theta_v}{\theta_{vc}} \tag{9}$$

where θ_v, the dimensionless reaction time, is given by

$$\theta_v = k_v (C_{Ao} - C_A^*) t$$

The fractional conversion of solid reactant, X, is found from

$$X = 1 - \left[\int_0^R 4\pi r^2 C_S dr \Big/ \int_0^R 4\pi r^2 C_{So} dr \right] \quad \text{as}$$

$$X = \frac{3}{(\phi'_v)^2} (\phi'_v \coth \phi'_v - 1) \cdot \frac{\theta_v}{\theta_{vc}} \tag{10}$$

The rate of reaction per particle, M_S, is found from $aM_S = M_A = 4\pi R^2 k_{mA} (C_{Ao} - C_{AS})$ as

$$aM_S = M_A = \frac{4\pi R C_{Ao} D'_{eA}}{\theta_{vc}} (\phi'_v \coth \phi'_v - 1) \tag{11}$$

The length of time for the first stage reaction to last is obtained from Equation (9) by letting $\xi = 1$ and $C_S = 0$ as

$$\theta_v = \theta_{vc} \tag{12}$$

As is evident from Equations (8) and (11), the concentration profile of component A and the rate of reaction per single particle are independent of time. Therefore, θ_{vc} can be regarded as the length of time (dimensionless) for the duration of the constant rate period. If the resistance to the liquid film diffusion around the particle is negligibly small, i.e. $N'_{Sh} = \infty$, then θ_{vc} becomes unity.

The solid reactant concentration distribution and the conversion at the end of the first stage can be found from Equations (9) and (10) as

$$\frac{C_S}{C_{So}} = 1 - \frac{\sinh(\phi'_v \xi)}{\xi \sinh \phi'_v} \tag{13}$$

$$X = \frac{3}{(\phi'_v)^2} \quad (\phi'_v \coth \phi'_v - 1) \qquad (14)$$

(b) The Second Stage Reaction

As the reaction progresses, as shown in Fig. 1, two zones appear; an outer zone in which the solid reactant is completely exhausted (the diffusion zone) and an inner zone where the reaction still takes place (the reaction zone). The material balance equations, the boundary conditions and the initial conditions for the second stage reaction are shown in the following table.

Inner Core (Reaction Zone)	Outer Layer (Diffusion Zone)
$0 = D'_{eA}\left(\frac{d^2C'_A}{dr^2} + \frac{2}{r}\frac{dC'_A}{dr}\right) - ak_vC_{So}(C'_A - C^*_A)$ (15)	$0 = D_{eA}\left(\frac{d^2C_A}{dr^2} + \frac{2}{r}\frac{dC_A}{dr}\right)$ (18)
$\frac{\partial C_S}{\partial t} = -k_vC_{So}(C'_A - C^*_A)$ (16)	$C_S = 0$ (19)
$\frac{dC'_A}{dr} = 0$ at $r = 0$ (17)	$D_{eA}\frac{dC_A}{dr} = k_{mA}(C_{Ao} - C_A)$ at $r = R$ (20)
$C'_A = C_A$ at $r = r_m$	
$D'_{eA}\frac{dC'_A}{dr} = D_{eA}\frac{dC_A}{dr}$ (21)	
$C_S = C_{So}\left[1 - \frac{\sinh(\phi'_v\xi)}{\xi \sinh \phi'_v}\right]$ at $t = t_c = \frac{\theta_{vc}}{k_v(C_{Ao} - C^*_A)}$ and $r_m = R$ (22)	

where r_m is the boundary of the two zones. The concentration distribution of A can be obtained from Equations (15), (17), (18), and (20) as

$$\frac{C'_A - C^*_A}{C_{Ao} - C^*_A} = \frac{C_{Am} - C^*_A}{C_{Ao} - C^*_A} \frac{\xi_m \sinh(\phi'_v \xi)}{\xi \sinh(\phi'_v \xi_m)} \quad \text{for } 0 \leq r \leq r_m \tag{23}$$

and

$$\frac{C_A - C^*_A}{C_{Ao} - C^*_A} = \frac{C_{Am} - C^*_A}{C_{Ao} - C^*_A} \cdot \frac{\xi_m}{\xi} \cdot \frac{1 - \xi + \xi/N_{Sh}}{1 - \xi_m + \xi_m/N_{Sh}} + \frac{1 - \xi_m/\xi}{1 - \xi_m + \xi_m/N_{Sh}} \tag{24}$$

$$\text{for } r_m \leq r \leq R$$

where $N_{Sh} = \frac{k_{mA} R}{D_{eA}}$, $\xi_m = \frac{r_m}{R}$ and C_{Am} is the concentration of A at the boundary of the two zones, or at $r = r_m$, and is obtained from Equation (21) as

$$\frac{C_{Am} - C^*_A}{C_{Ao} - C^*_A} = \frac{1}{1 + \frac{D'_{eA}}{D_{eA}} \left(1 - \xi_m + \frac{\xi_m}{N_{Sh}}\right)[\phi'_v \xi_m \coth(\phi'_v \xi_m) - 1]} \tag{25}$$

In Fig. 4, the variation of C_{Am} is shown as a function of ϕ_v ($= \phi'_v$) when $N_{Sh} = \infty$ and $D_{eA} = D'_{eA}$. As the values of ϕ_v become larger, $C_{Am} - C^*_A$ is seen to approach zero. This corresponds to the condition of the fast chemical reaction and the slow diffusion through solid with the solid diffusion being the rate controlling factor. The variation in solid reactant concentration can be found from

$$C_S = (C_S)_{t_c} - \int_{t_c}^{t} k_v C_{So} (C'_A - C^*_A)\, dt, \text{ as}$$

$$\frac{C_S}{C_{So}} = 1 - \frac{\sinh(\phi'_v \xi)}{\xi \sinh \phi'_v} - \frac{\sinh(\phi'_v \xi)}{\xi} \int_{\theta'_{vc}}^{\theta_v} \frac{[\xi_m / \sinh(\phi'_v \xi_m)]\, d\theta_v}{1 + \frac{D'_{eA}}{D_{eA}}[1 - \xi_m + \frac{\xi_m}{N_{Sh}}][\phi'_v \xi_m \coth(\phi'_v \xi_m) - 1]} \tag{26}$$

The integration in Equation (26) requires the relation between θ_v and ξ_m. This can be found as follows. Differentiating Equation (26) with respect to θ_v at $\xi = \xi_m$ and $C_S = 0$, we obtain,

$$\frac{d\theta_v}{d\xi_m} = -\frac{1}{\xi_m}[\phi'_v \xi_m \coth(\phi'_v \xi_m) - 1][1 + \frac{D'_{eA}}{D_{eA}}(1 - \xi_m + \xi_m/N_{Sh}) \cdot \{\phi'_v \xi_m \coth(\phi'_v \xi_m) - 1\}] \quad (27)$$

Thus, the time required for the ash layer to reach r_m is obtained as

$$\theta_v = \theta_{vc} + \int_1^{\xi_m} \frac{d\theta_v}{d\xi_m} d\xi_m$$

Ausman and Watson (1) used the graphical method to obtain the above integration for $D_{eA} = D'_{eA}$. However, an analytical solution can be obtained as follows:

$$\theta_v = 1 + (1 - \frac{D'_{eA}}{D_{eA}}) \ln \frac{\xi_m \sinh\phi'_v}{\sinh(\phi'_v \xi_m)} + \frac{\phi_v^2}{6}(1 - \xi_m)^2 \cdot (1 + 2\xi_m)$$

$$+ \frac{D'_{eA}}{D_{eA}}(1 - \xi_m)[\phi'_v \xi_m \coth(\phi'_v \xi_m) - 1] + \frac{1}{N_{Sh}} \cdot \frac{\phi_v^2}{3}(1 - \xi_m^3)$$

$$+ \frac{\xi_m}{N'_{Sh}}[\phi'_v \xi_m \coth(\phi'_v \xi_m) - 1] \quad (28)$$

The time required for the reaction to complete both the first stage and the second stage, θ^*_v, can be found from the above equation by letting $\xi_m = 0$ as

$$\theta^*_v = 1 + \frac{\phi_v^2}{6}(1 + \frac{2}{N_{Sh}}) + (1 - \frac{D'_{eA}}{D_{eA}}) \ln \frac{\sinh\phi'_v}{\phi'_v} \quad (29)$$

Substituting Equation (28) into Equation (26), the concentration distribution for solid reactant is obtained as

$$\frac{C_S}{C_{So}} = 1 - \frac{\xi_m \sinh(\phi'_v \xi)}{\xi \sinh(\phi'_v \xi_m)} \quad (30)$$

and the solid reactant conversion is

$$X = 1 - \xi_m^3 + \frac{3\xi_m}{(\phi_v')^2}\left[\phi_v'\xi_m \coth(\phi_v'\xi_m) - 1\right] \tag{31}$$

Thus, we have completed the derivation of the general model for a solid-liquid reaction in a spherical particle. Next, we shall introduce the effectiveness factor, η_v for this reaction so that the effect of diffusion can be more conveniently examined. Accordingly, the effectiveness factor η_v for solid-liquid reaction is defined as

$$\eta_v = \frac{\text{Actual reaction rate}}{\text{Reaction rate obtainable when the concentration and temperature exist in the interior of the particle are the same as that exist in the bulk phase.}}$$

Unlike the effectiveness factor used in catalytic reactions which is based on the concentration and temperature at the surface of the catalysts, the effectiveness factor for solid-liquid reaction is based on the concentration and temperature in the bulk liquid phase which do not change during the reaction. Hence,

$$\eta_v = \frac{\int k_v C_{So}(C_A' - C_A^*)dV}{\int k_v C_{So}(C_{Ao} - C_A^*)dV}$$

and is given as

The First Stage:

$$\eta_v = \frac{3}{(\phi_v')^2}\left[\phi_v' \coth \phi_v' - 1\right] \cdot \frac{1}{\theta_{vc}} \tag{33}$$

The Second Stage:

$$\eta_v = \frac{3}{(\phi_v'\xi_m)^2} \cdot \frac{\phi_v'\xi_m \coth(\phi_v'\xi_m) - 1}{1 + \frac{D_{eA}'}{D_{eA}}\left[1 - \xi_m + \xi_m/N_{Sh}\right]\left[\phi_v'\xi_m \coth(\phi_v'\xi_m) - 1\right]} \tag{34}$$

The effectiveness factor as given in Equations (33) and (34) is equivalent to the ratio of the chemical reaction resistance to the total resistance consisting of the diffusional resistance and the chemical reaction resistance.

The Homogeneous Model ($D_{eA} = D'_{eA}$)

If we let $D_{eA} = D'_{eA}$ in the general model discussed in the previous section, we obtain the homogeneous model. Fig. 5 shows the relation between the reaction time and the solid reactant conversion, for various values of $\phi_v (= \phi'_v)$, in the case where the liquid-film resistance is negligibly small, i.e. $N_{Sh} = \infty$, As ϕ_v is increased, the diffusion of A through the solid becomes the rate-controlling factor and the lines converge into one line. Under this condition, Equations (23), (24), (28), and (31) are reduced to

$$C_A = C_A^* \qquad \text{for } 0 \le r \le r_m$$

$$\frac{C_A - C_A^*}{C_{Ao} - C_A^*} = \frac{1 - \xi_m/\xi}{1 - \xi_m + \xi_m/N_{Sh}} \qquad \text{for } r_m \le r \le R$$

$$X = 1 - \xi_m^3$$

and

$$\frac{\theta_v}{\theta_v^*} = 1 - 3(1 - X)^{2/3} + 2(1 - X)$$

Also from Equation (29), $\theta_v^* \propto R^2$.

These results are exactly the same as that obtainable from the unreacted-core shrinking model under a pseudo-steady state assumption when the ash diffusion is the rate-controlling factor. Therefore, when the diffusion through the solid is rate controlling, there is no way to distinguish from experimental data which

of the two models is the correct model for the given system.

On the other hand, if the chemical reaction is very slow, and is the rate controlling factor, ϕ_v approaches zero and

$$C_A' = C_{Ao} \qquad \text{for } 0 \leq r \leq R$$

$$\frac{C_S}{C_{So}} = 1 - \frac{\theta_v}{\theta_v^*}$$

$$X = \theta_v/\theta_v^* \qquad \text{and } \theta_v^* \propto R^0 \text{ (independent of R).}$$

As shown in Fig. 5, the relation between X and θ_v/θ_v^* is not greatly different from that of the unreacted-core shrinking model and therefore determination of a correct model from the experimental data is rather difficult.

For a clear demonstration of the difference between the two models, the rate of reaction is plotted against the solid reactant conversion as shown in Fig. 6. In Fig. 7, the relation between the effectiveness factor and the conversion obtained from Equations (33) and (35) is shown. As the values of ϕ_v are increased above one, the effectiveness factor becomes smaller moving towards the diffusion controlled region. However, at complete conversion (X= 1), η_v becomes unity for all ϕ_v returning to the chemical reaction controlled region. In Fig. 8, the effect of liquid-film diffusion is shown for ϕ_v = 2 and 20. As N_{Sh} becomes smaller than 100, the effect becomes apparent, becoming particularly significant during the first stage reaction.

The Unreacted-Core Shrinking Model ($D'_{eA} \ll D_{eA}$)

Next, we consider the case where D'_{eA} is very much smaller than D_{eA}. Under this condition, ϕ'_v becomes large so that $\ln[\xi_m \sinh\phi'_v/\sinh(\phi'_v \xi_m)]$ can be approximated by $\phi'_v(1 - \xi_m)$. Also, since $\frac{D'_{eA}}{D_{eA}}$ is small, Equations (28) and (31) become

$$\frac{\theta_v}{\phi'_v} = 1 - \xi_m + \frac{\phi_v}{2}\sqrt{\frac{D'_{eA}}{D_{eA}}}\,(1 - \xi_m^2) + \frac{\phi_v}{3}\sqrt{\frac{D'_{eA}}{D_{eA}}}\,\left(\frac{1}{N_{Sh}} - 1\right)(1 - \xi_m^3) \qquad (35)$$

$$X = 1 - \xi_m^3 \qquad (36)$$

These equations are equivalent to the equations derived based on the unreacted-core shrinking model under a pseudo-steady state assumption:

$$\theta_S = 1 - \xi_c + \frac{\phi_S}{2}(1 - \xi_c^2) + \frac{\phi_S}{3}\left(\frac{1}{N_{Sh}} - 1\right)(1 - \xi_c^3) \qquad (37)$$

$$X = 1 - \xi_c^3 \qquad (38)$$

where $\phi_S = \dfrac{Rak_s C_{So}}{D_{eA}}$ and $\theta_S = \dfrac{k_s(C_{Ao} - C^*_A)\,t}{R}$

Here $\xi_m (= r_m/R)$ is equivalent to $\xi_c (= r_c/R)$ for the unreacted-core shrinking model, and k_s is the reaction rate constant based on the reaction surface of the shrinking core.

The similarity of the two models when ϕ'_v is large can be realized from Fig. 3 in which $(C'_A - C^*_A)$ becomes nearly zero in the reaction zone for ϕ'_v larger than 100, indicating no penetration of gas A into the shrinking core. Comparing Equations (35) and (36) with Equations (37) and (38), we can relate the surface-based quantities, k_s, ϕ_S, and θ_S to the volume-based quantities k_v, ϕ_v, and θ_v as

$$\phi_S = \phi_v \sqrt{\frac{D'_{eA}}{D_{eA}}} \quad , \quad \theta_s = \theta_v / \phi'_v \text{ and } k_s = \sqrt{\frac{D'_{eA} k_v}{a C_{So}}} \tag{39}$$

The difficulties associated with the determination of a proper model for a solid-liquid reaction system from experimental data can be realized from Equation (39) in which k_s is proportional to $\sqrt{k_v}$, therefore, the activation energy obtained based on the unreacted-core shrinking model could be as small as 1/2 of the true value. It was also pointed out in the previous section that the shapes of curves relating conversion and time are so similar for the various models (shown in Fig. 5), this criterion alone is not sufficient to determine the prevailing mechanism. It is hoped that the study presented here will be useful in the explanation of the mechanism of solid-liquid water pollution systems.

CONCLUSION

An analytical solution under the pseudo steady state assumption, is obtained for a general model of solid-liquid reactions taking place in a single particle. This model is represented by the first stage and the second stage reaction with the second stage being characterized by the diffusion through an ash layer and the reaction in an inner core. The effective diffusivities for the two zones, D_{eA} and D'_{eA} are considered different but are constant during the course of reaction. The effectiveness factors are also defined for solid-liquid reactions and the effects of diffusion are examined. The general model is shown to become the homogeneous model when $D_{eA} = D'_{eA}$ and the unreacted-core shrinking model when $D_{eA} >> D'_{eA}$. The two rate constants involved in the expressions of these models, are related by

$$k_s = \sqrt{\frac{D'_{eA} k_v}{a C_{So}}}$$

It was also found that the unreacted-core shrinking model is valid for $\phi'_v > 100$. Some experimental difficulties involved in selecting a proper model for analysis of data are also discussed.

Notation

a	Stoichiometric coefficient	--
C_A	Concentration of component A in gas, C_A' in reaction zone, C_{Ao} in bulk phase, C_{Am} at boundary between reaction zone and ash layer, C_{As} at outer surface of particle	Moles/L^3
C_A^*	Equilibrium concentration of component A	Moles/L^3
C_S	Concentration of solid reactant, S	Moles/L^3
C_{So}	Initial concentration of solid reactant	Moles/L^3
D_{eA}	Effective diffusivity of component A in ash layer	L^2/θ
D'_{eA}	Effective diffusivity of component A in reaction zone	L^2/θ
k_{mA}	Mass transfer coefficient	L/θ
k_s	Reaction rate constant based on area	$L^4/(\text{Moles } \theta)$
k_v	Reaction rate constant based on volume	$L^3/(\text{Moles } \theta)$
M_A	Total reaction rate of component A	Mole/θ
M_S	Total reaction rate of component S	Mole/θ
R	Particle radius	L
r	Distance from the center of sphere	L
r_m	r at boundary between reaction zone and ash layer	L
r_c	Distance from the center of sphere to unreacted core surface	L
$N_{Sh} = \frac{k_{mA}R}{D_{eA}}$		--
$N'_{Sh} = \frac{k_{mA}R}{D'_{eA}}$		--
t	Time	θ
t^*	Time for complete conversion, t_c time for completion of first stage reaction	θ
V	Volume	L^3
X	Conversion	--

η_v	Effectiveness factor	--
θ_v	Dimensionless time	--
	θ_{vc} for complete reaction of the first stage, θ_v^* for complete reaction of both stages.	
ξ	Dimensionless radius, $\xi = \frac{r}{R}$, $\xi_m = \frac{r_m}{R}$	--
ϕ_v	Thiele modulus based on D_{eA}	--
	ϕ_v' based on D_{eA}'	
ε	voidage	--

REFERENCE

1) Ausman, J. M. and C. C. Watson, Chem. Eng. Sci., 17, 323 (1962).

2) Yagi, S. and D. Kunii, Fifth Symposium (International) on Combustion, 231 (1955).

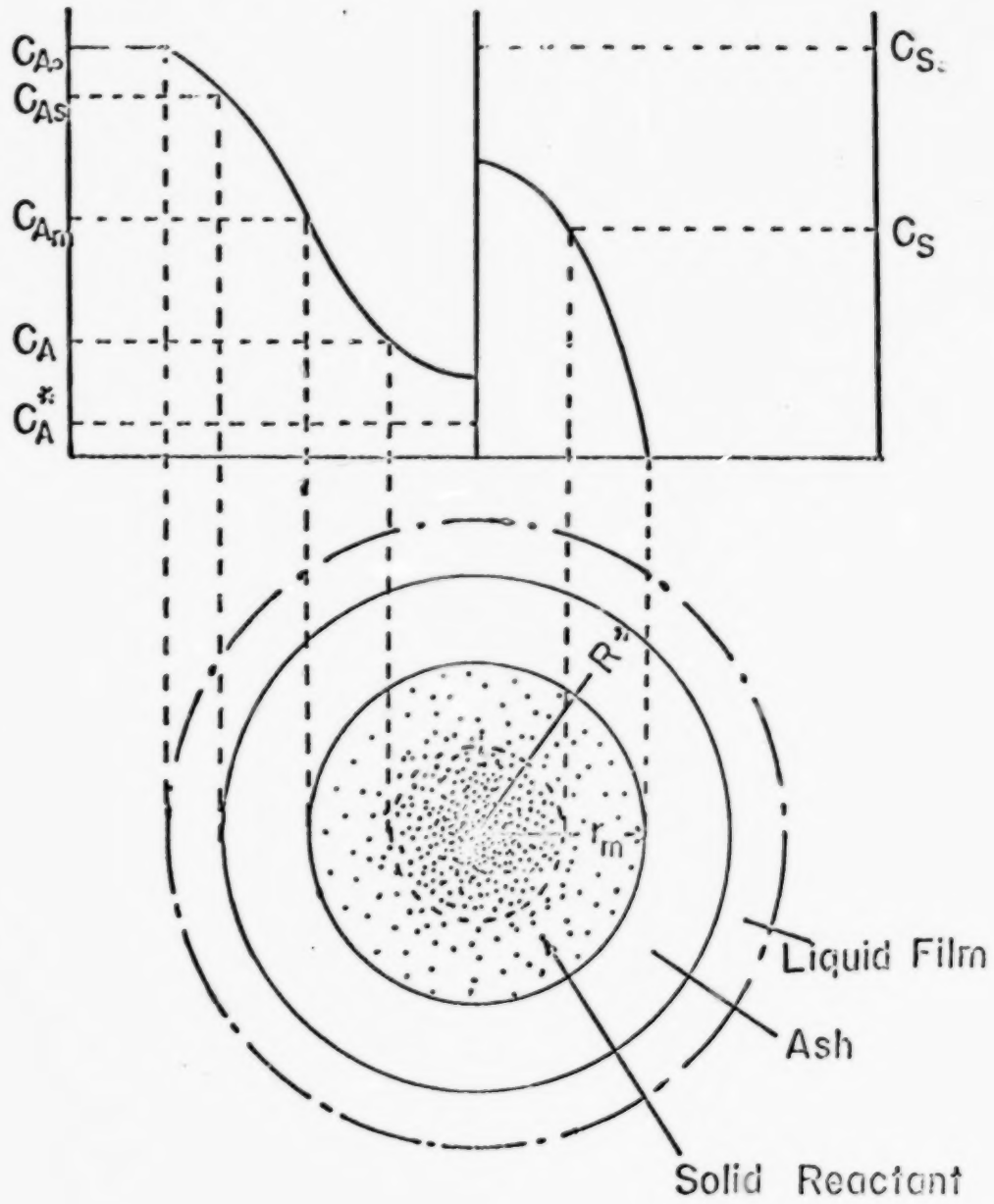

Fig. 1 Schematic diagram of concentration profile in the second stage.

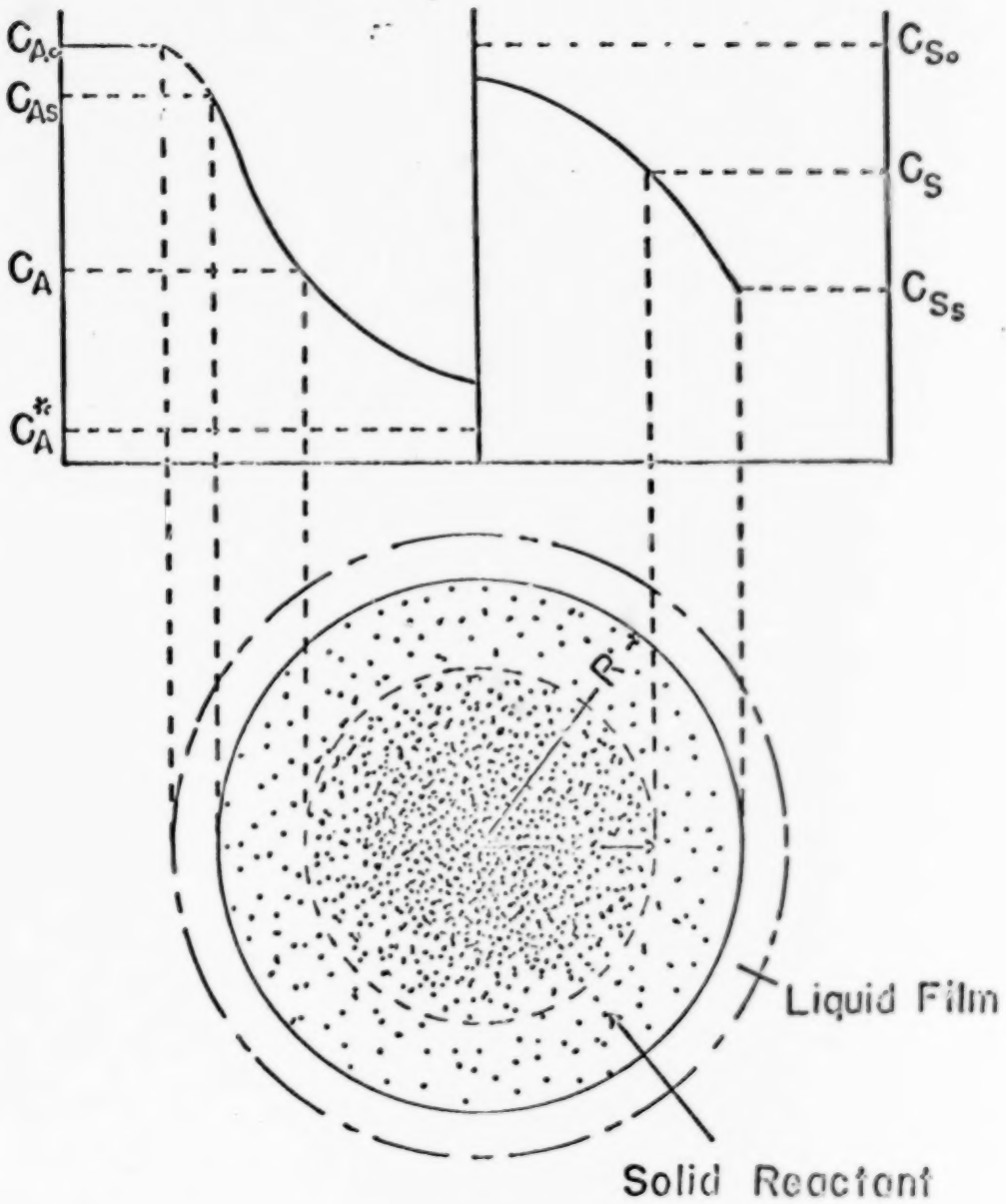

Fig. 2 Schematic diagram for concentration profile in the first stage.

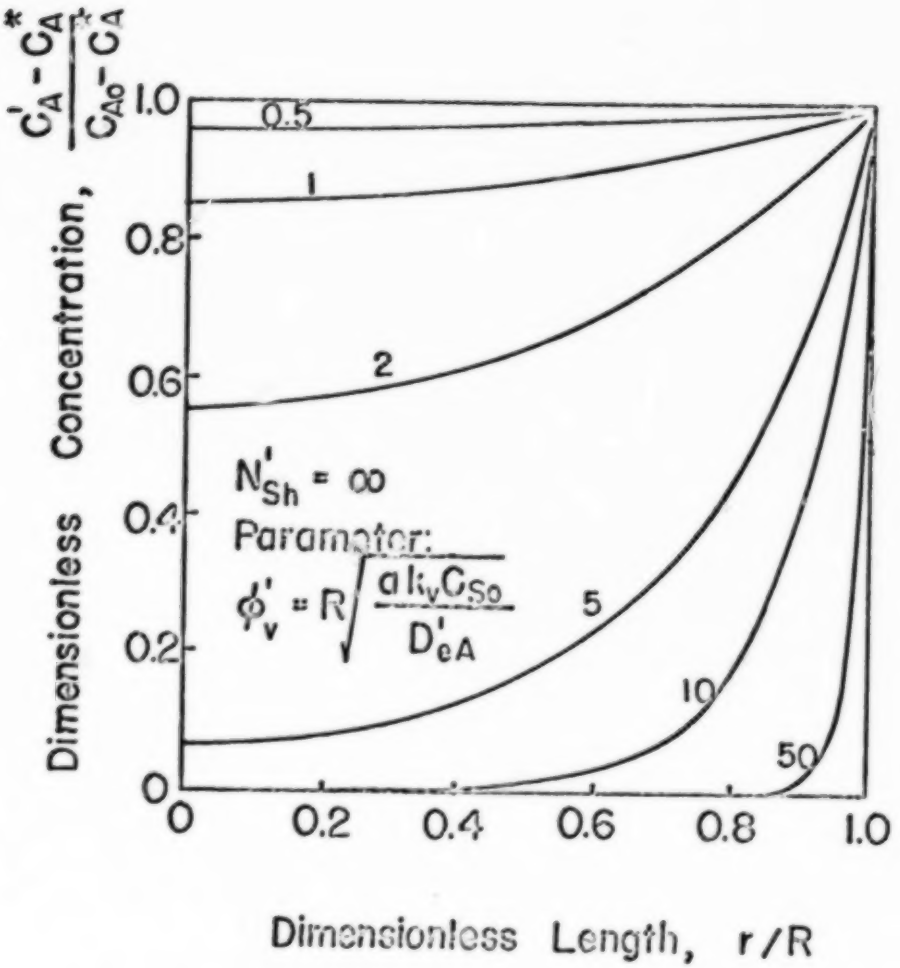

Fig. 3 Influence of parameter, ϕ'_v, on concentration profile of component A.

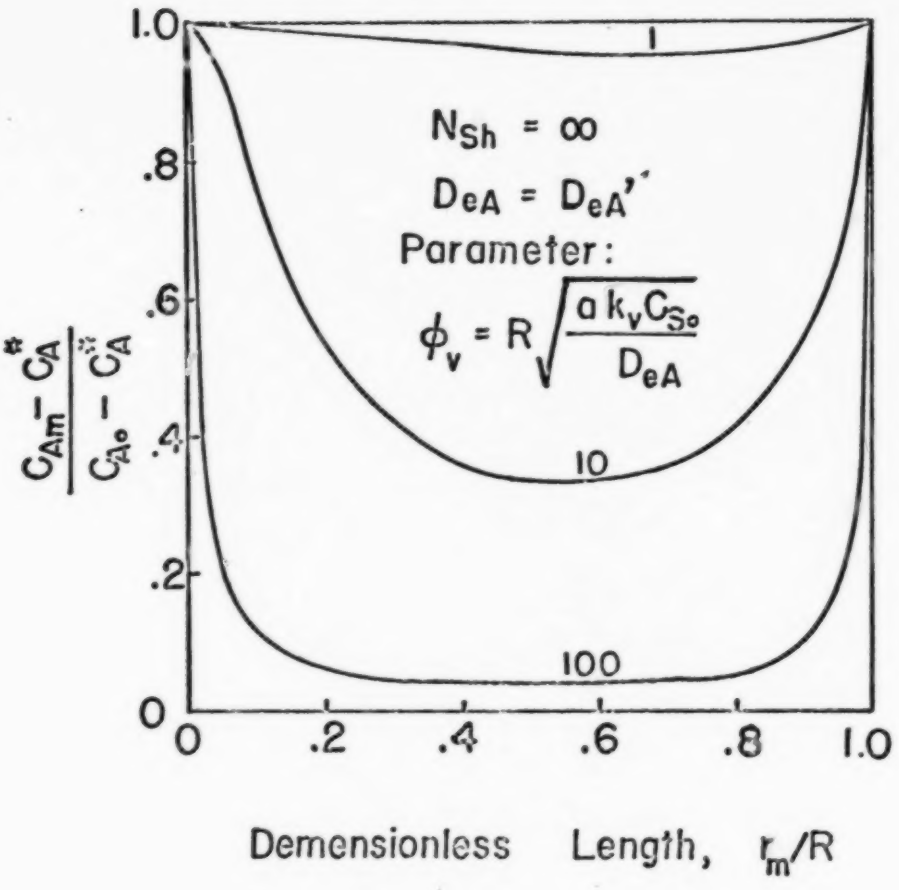

Fig. 4 Influence of ϕ_v on C_{Am}, the concentration of component A at the boundary.

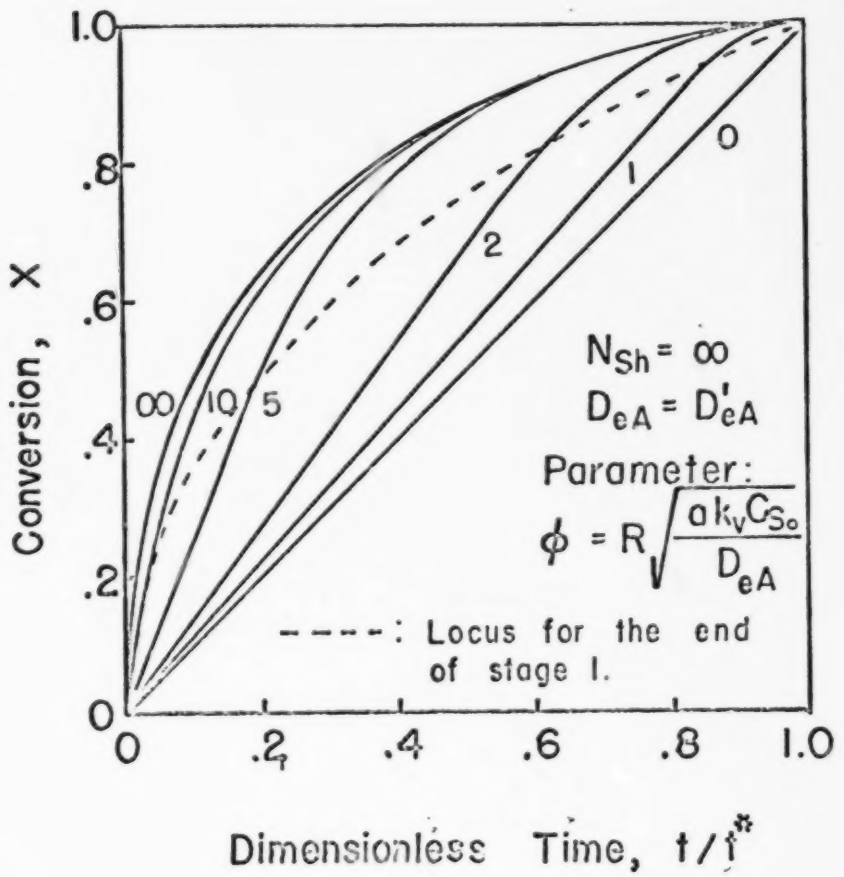

Fig. 5 Fractional conversion of solid reactant as a function of dimensionless time for homogeneous model (sphere).

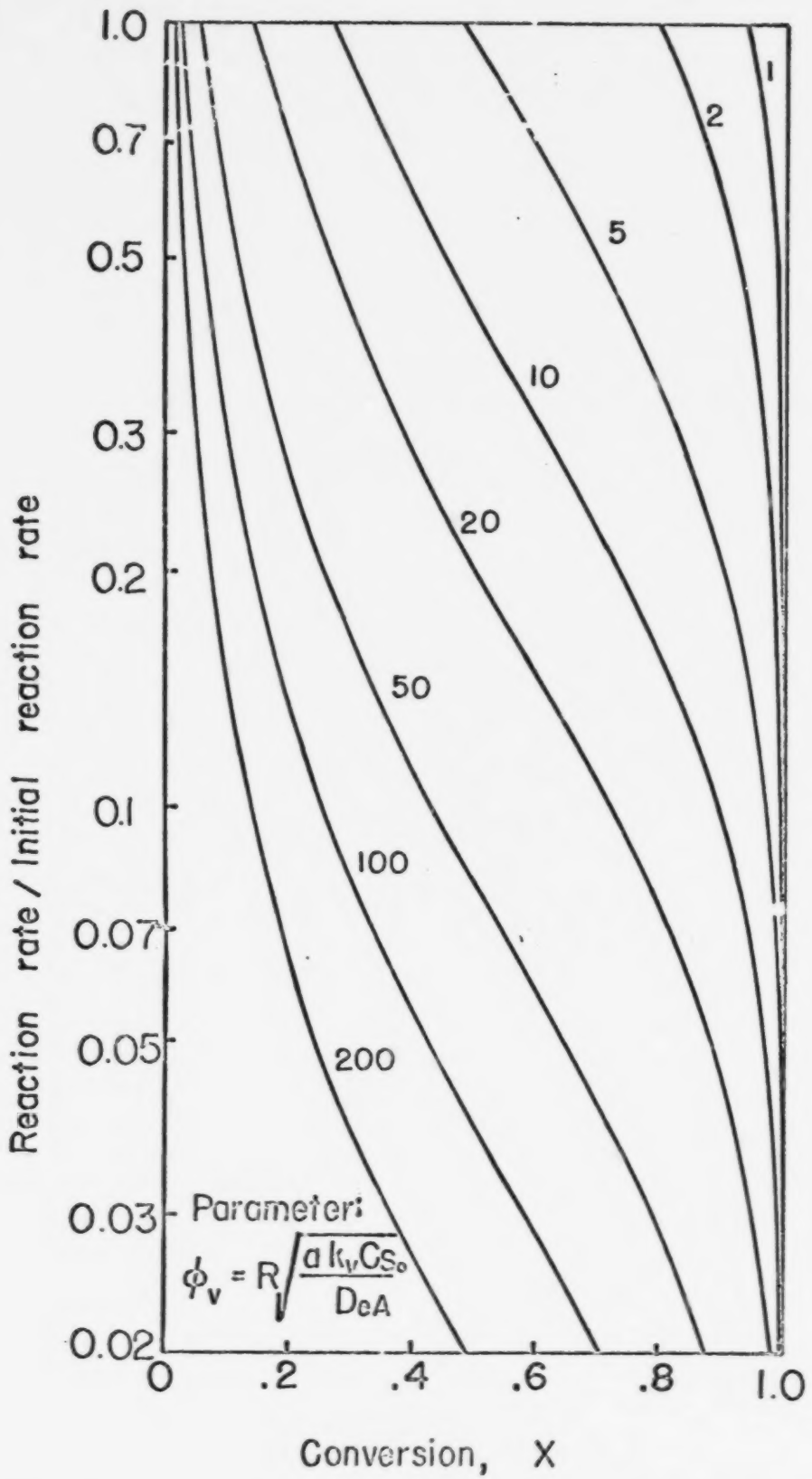

Fig. 6 Relation between conversion and reaction rate for $N_{Sh} = \infty$ and $D_{eA} = D'_{eA}$.

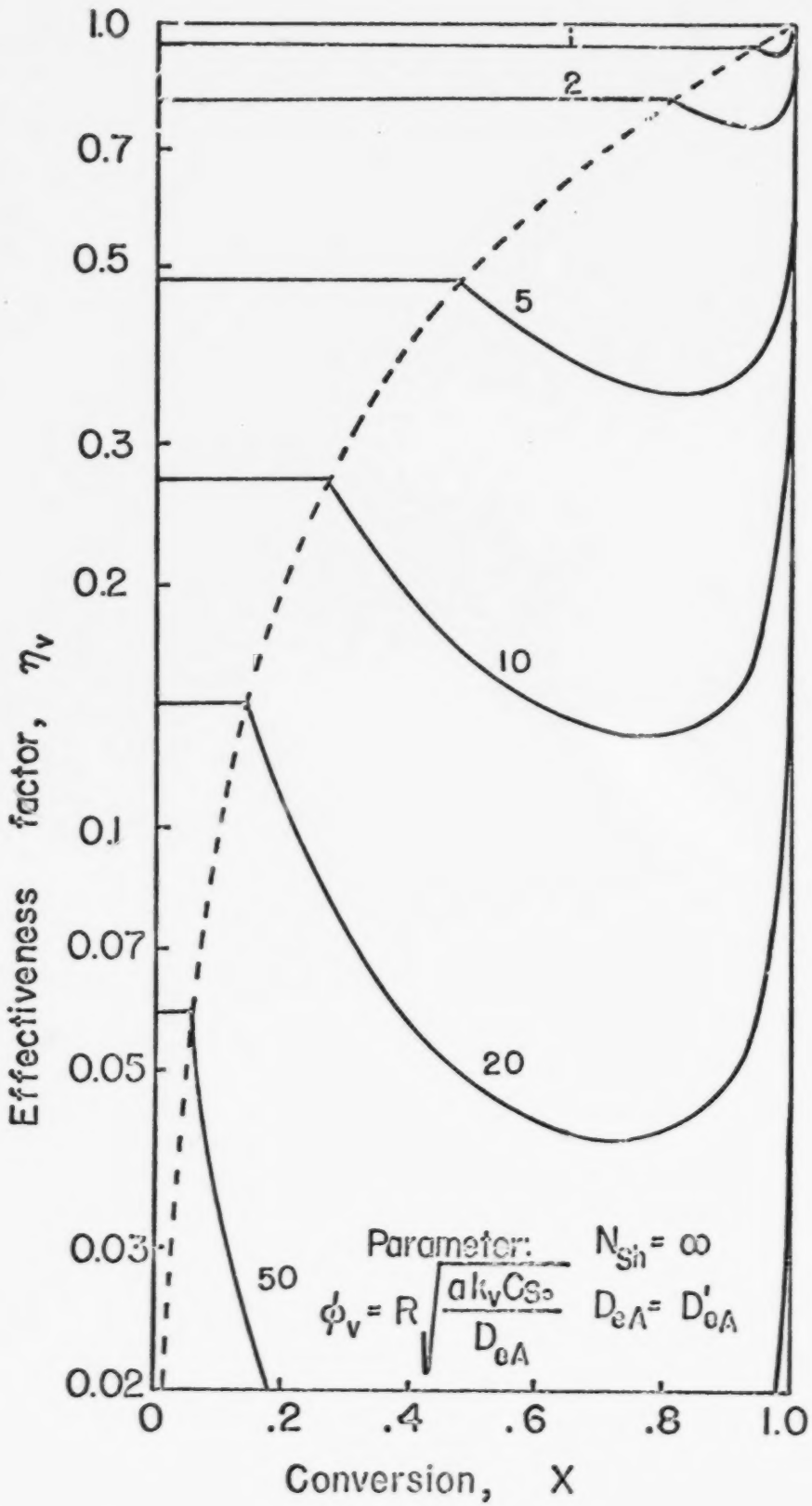

Fig. 7 Effect of ϕ_v on effectiveness factor